SUPPLEMENTARY INFORMATION

Multifunctional electromechanical and thermoelectric polyaniline-poly(vinyl acetate) latex composites for wearable devices

Laura Horta Romarís[1], M. Victoria González Rodríguez[1], Bincheng Huang[2], P. Costa[3,4], Aurora Lasagabáster Latorre[1,5], S. Lanceros-Mendez[6,7], María José Abad López[1]*

[1] *Grupo de Polímeros, Centro de Investigacións Tecnolóxicas, Universidade da Coruña, Campus de Ferrol, 15471 Ferrol, Spain.*

[2] *Dpt of Automobile Engineering, School of Transportation Science and Engineering, Beihang University, Beijing, 100191, China*

[3] *Centre of Physics, University of Minho, 4710-057 Braga, Portugal*

[4] *Institute for Polymers and Composites IPC/I3N, University of Minho, 4800-058 Guimarães, Portugal*

[5] *Dpto Química Orgánica I, Facultad de Óptica, Universidad Complutense de Madrid, Arcos de Jalón 118, 28037Madrid, Spain.*

[6] *BCMaterials, Basque Center for Materials, Applications and Nanostructures, UPV/EHU Science Park, 48940 Leioa, Spain*

[7] *IKERBASQUE, Basque Foundation for Science, 48013 Bilbao, Spain*

**Corresponding author mjabad@udc.es*

S1. EXPERIMENTAL

S1.1. Molecular weight of PANI

The molecular weight of PANI base is determined from its intrinsic viscosity [η], according to the Mark-Houwink-Sakurada equation:

$$[\eta] = K.M_{\eta}^{\alpha} \qquad (S1)$$

where K and α are constants for a particular polymer–solvent pair at a particular temperature. Poly(p-phenylene terephthalamide) has a rigid chain with conjugated double bonds similar to PANI. Therefore, in a first approximation the values of K = 1.95×10^{-6} and α= 1.36, characteristic of this polymer in H_2SO_4 medium, were used for PANI[1]. The estimated molecular weight of the PANI base is 6,300 Da (R^2 = 0.97).

S1.2. Measurement of the Seebeck coefficient

The home-made device used to measure the Seebeck coefficient is presented in Fig. S1. Once the base temperature has been stabilized, a voltage (20 mA) is applied to the 300 Ω heater to produce a thermal gradient through the sample. Fig. S2A shows that the thermoelectric voltage is very stable before applying the voltage to the heater. This is achieved by stabilizing the temperature for a couple of hours, so that the gradient inside the sample is less than 1 mK. This is an important factor for obtaining reliable measurements. Upon heating, the thermoelectric voltage increases progressively up to a thermal gradient of ≈2.5K. At this moment, the heater is switched off and the relaxing voltage is monitored as the thermal gradient decreases. In Fig. S2B the lineal adjustment between the voltage and thermal difference between the edges of the sample can be observed. The slope of the curve is the Seebeck coefficient.

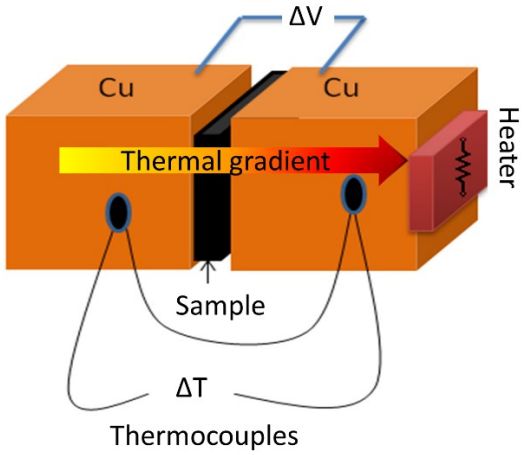

Fig.S1. Scheme of the home-made device that measures the Seebeck coefficient.

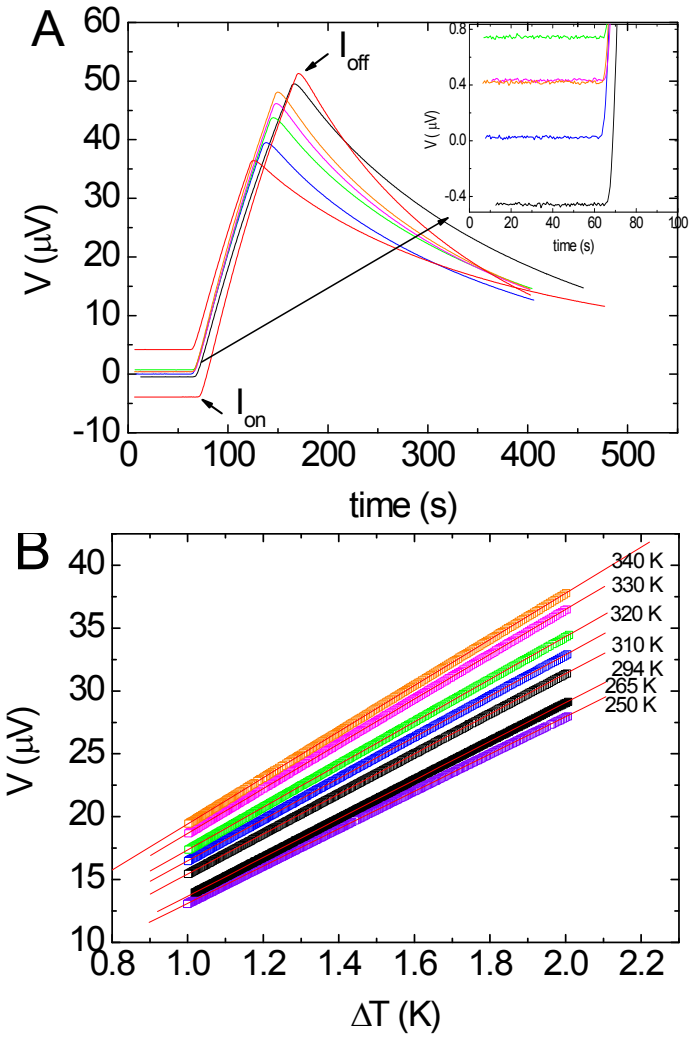

Fig.S2. Voltage before and after applying current (A) and adjustment of voltage curves after applying thermal gradient (B).

S2. RESULTS

S2.1. FTIR

The carbonyl band is used to characterize the amount of PVAc bound to the NH groups of PANI by analyzing the vibrations of free ($\nu_{C=O}$) and bound ($\nu_{C=O\text{--}HN}$) carbonyl groups. After subtraction of the baseline, the intensity of the two peaks at 1730 and 1715 cm^{-1}, respectively, is estimated by fitting two Gaussians to the data (Fig.S3B).

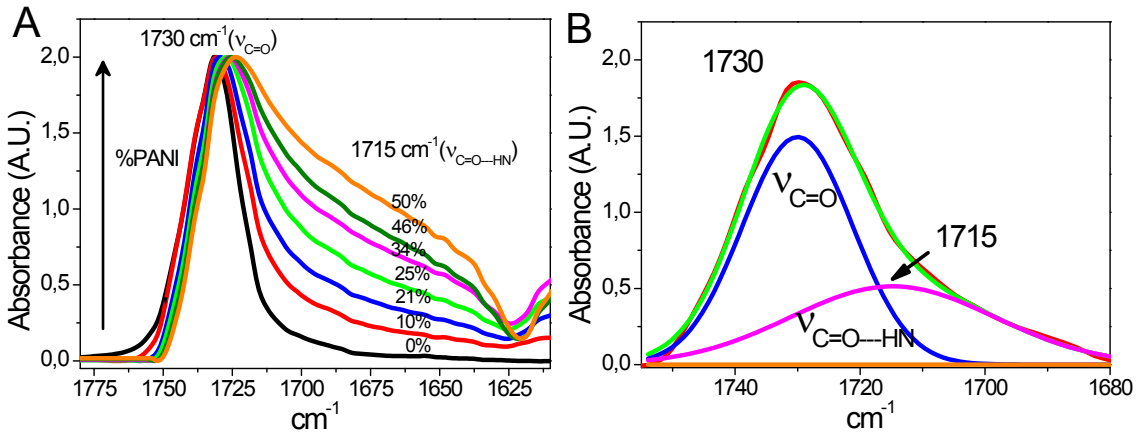

Figure S3. A) Carbonyl region of the FTIR absorption spectra of composites of increasing PANI concentration. The intensities of the spectra are normalized with respect to the peak of free C=O; B) Fit of two Gaussians to the data for the *P30L70* film. The areas under the two peaks are assigned to bound ($\nu_{C=O\cdots HN}$) and free ($\nu_{C=O}$) carbonyl groups.

The areas under the peak correspond to the relative amount of $C{=}O_{bound}$ (A_b) and $C{=}O_{free}$ (A_f). Nevertheless, here the fraction of H-bonded carbonyl groups (f_b) is roughly calculated by Eq. S2, where *a* is the ratio of the molar absorption coefficients. A value of 1.5 was taken for the *a* ratio, according to previous studies[2].

$$f_b = \frac{A_b/a}{A_b/a + A_f} \quad (S2)$$

From another point of view, the locations of the δ_{NH^+}, Q and B bands are indicative of the doping level of PANI[3,4]. At low PANI contents, the band maxima are observed at higher wavenumbers compared to pure PANI. On increasing the PANI content, the bands δ_{NH^+} and B gradually downshift to wavenumbers similar to pristine PANI (Fig. S4A-B). Concerning the Q band, it is located at higher wavenumbers than pure PANI for composites with PANI contents below 34% (shifting from 1575 to 1565 cm^{-1} on increasing PANI from 5 to 25 %wt.); it further downshifts to 1556 cm^{-1} in the range spanning from 34 to 46% wt and finally, decreases to 1541 cm^{-1} for PANI contents ≥50 %wt (Fig. S4A). At PANI loadings below 30 % wt, a probable partial deprotonation may explain the band locations. A gradual increase in the doping level, along with H-bonding with PVAc, accounts for further downshift [5].

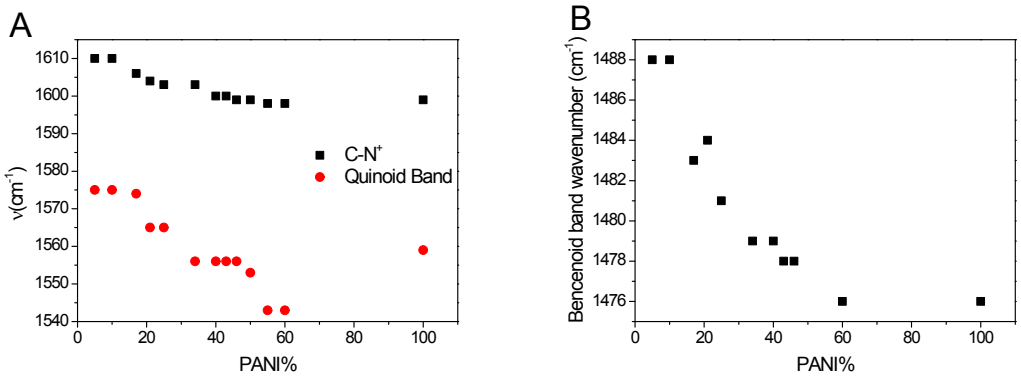

Figure S4. Shifts of PANI FTIR bands upon increasing the PANI %wt in PANI-PVAc composites: A) wanumbers of the δ_{NH^+} (squares) and Quinoid band (Q) (circles) and B) bencenoid band (B).

S2.2. XRD

The XRD pattern of neat PANI exhibits partial crystallinity with characteristic reflections at 2θ = 9.3, 15.1, 20.5, 25.6, 27.1 and 30.0° and a broad asymmetric scattering of the amorphous phase. These structural features are indicative of the orthorhombic structure of ES-I type. The most intense reflection at 2θ = 25.6° is due to periodicity perpendicular to the polymer chain [6].

The same PANI features are observed for composites with PANI contents ≥ 17% wt. In order to evaluate the PANI phase contribution in the composite films, the normalized diffractogram of amorphous PVAc was subtracted from the normalized composites patterns. The obtained difference patterns were used to estimate the degree of crystallinity of the PANI phase (X_c). The intensities of the peak at 2θ= 25.6º, the crystallite sizes (L), estimated from the widths of the peak at 25.6°, and X_c are presented in Table S1.

Table S1. Intensity of the peak at 2θ= 25.6º, crystallite size (L) estimated from the width of the peak at 25.6° and degree of crystallinity (X_c) of the PANI phase within the composites.

PANI (wt %)	Intensity	L(x10^{-10} m)	X_c (%)
17	0.011	-	19
21	0.021	-	24

25	0.015	-	23
34	0.024	29.8	30
40	0.033	34.2	37
43	0.033	47.6	39
46	0.035	51.3	37
55	0.057	60.4	48
100	0.068	57.3	57

S2.3. Mechanical properties

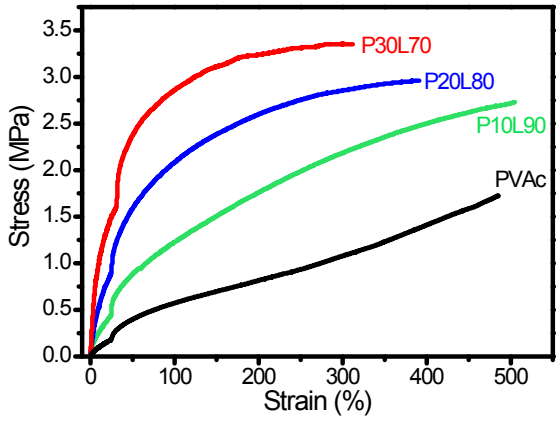

Fig. S5. Stress-strain curves until rupture of pure PVAc and PANI-PVAc composites: *P10L90*, *P20L80* and *P30L70*

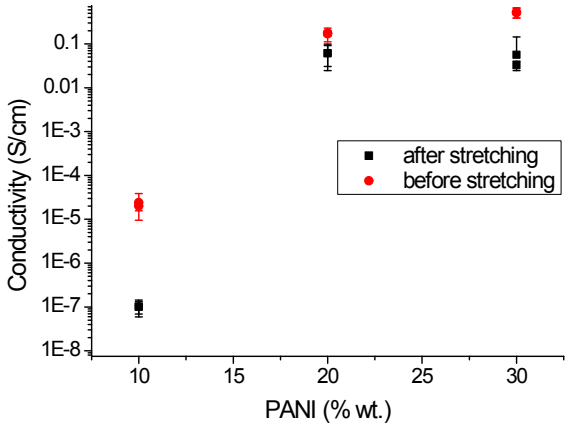

Figure. S6. Changes in conductivity of *P10L90*, *P20L80* and *P30L70* composites after tensile testing.

S2.4. Thermal stability

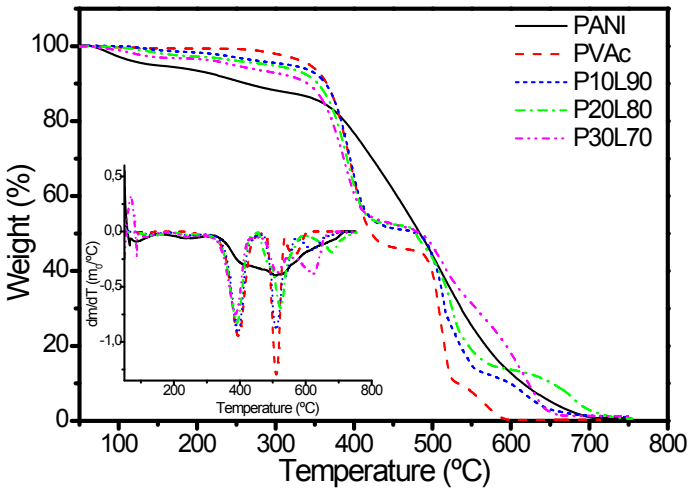

Fig. S7. TGA and DTG (inset) curves of PANI-HCl, PVAc and PANI-PVAc composites: *P10L90, P20L80* and *P30L70*.

References

1 J. Yang and B. Weng, *Synthetic Metals*, 2009, **159**, 2249–2252.

2 S.-W. Kuo, S.-C. Chan and F.-C. Chang, *Polymer*, 2002, **43**, 3653–3660.

3 M. Trchová, I. Šeděnková, E. Tobolková and J. Stejskal, *Polymer Degradation and Stability*, 2004, **86**, 179–185.

4 L. Horta-Romarís, M.-J. Abad, M. V. González-Rodríguez, A. Lasagabáster, P. Costa and S. Lanceros-Mendez, *Materials & Design*, 2016, **114**, 288–296.

5 N. Y. Yuan, F. F. Ma, Y. Fan, Y. B. Liu and J. N. Ding, *Composites Part A: Applied Science and Manufacturing*, 2012, **43**, 2183–2188.

6 J. P. Pouget, M. E. Jozefowicz, A. J. Epstein, X. Tang and A. G. MacDiarmid, *Macromolecules*, 1991, **24**, 779–789.